Efficient Gabor Filter Design Using Rician Output Statistics

Thomas P. Weldon
The Pennsylvania State University
201 Electrical Engineering East
University Park, PA, U.S.A. 16802
tpw@ruth.ece.psu.edu

William E. Higgins
The Pennsylvania State University
206 Electrical Engineering East
University Park, PA, U.S.A. 16802
weh@ruth.ece.psu.edu

Dennis F. Dunn
The Pennsylvania State University
103 Pond Laboratory
University Park, PA, U.S.A. 16802
dunn@cse.psu.edu

ABSTRACT

Gabor filters have been applied sucessfully to a broad range of multidimensional signal processing and image processing tasks. The present paper considers the design of a single filter to segment a two-texture image. A new efficient algorithm for Gabor-filter design is presented. The algorithm draws upon previous results that showed that the output of a Gabor-filtered texture is well represented by a Rician distribution. The new algorithm uses the Rician model to estimate the output statistics of a pair of sample textures from their windowed autocorrelation functions. A measure of the total output power is used to select the center frequency of the filter and estimate the output statistics. The method is further generalized to include the statistics of post-filtered outputs. Experimental results are presented that demonstrate the efficacy of the algorithms.

INTRODUCTION

[1] Gabor filters have been successfully applied to many imaging and multidimensional signal processing applications, such as document analysis [1, 2] and image texture segmentation [3, 4, 5]. An advantage of these filters is that they satisfy the minimum space-bandwidth product per the uncertainty principle. Hence, they provide simultaneous optimal resolution in both the space and spatial-frequency domains [6]. Further, they are bandpass filters, conforming well to the human visual system's robust capabilities [6]. Generally speaking, Gabor filters are employed to solve problems involving structurally complex textured images. We consider the problem of segmenting textured images in this paper.

We propose a new algorithm for efficiently designing Gabor filters. The algorithm, since it is based on the statistical characteristics of the filtering process, also enables one to predict the expected performance of the designed filters. Overall, our methodology gives greater insight into the Gabor-filter design process than has previously been discussed. Our methods focus on the problem of designing a single filter that discriminates between two different textures. But they can be generalized to the multi-texture case, as we briefly discuss.

A central issue in applying these filters to texture segmentation is the determination of the filter parameters. Jain and Farrokhnia considered a filter-bank scheme, but the filters were predetermined ad hoc, *not designed* [2]. One difficulty with this approach is that the filter parameters are preset and are not necessarily optimal for a particular processing task. Recent work by Bovik presented an approach that uses one Gabor filter per texture [3], and Dunn and Higgins provided a detailed treatment of the optimal design of a single Gabor filter to segment two textures [4].

This paper further considers the issue of designing a single Gabor filter for discriminating between two textures (the texture segmentation problem). The following section first reviews the assumed signal-processing framework. Next we propose a Gabor-filter design technique, based on autocorrelation measurements, that is more efficient computationally than [4]. Then, using an input signal model, we estimate the mean and variance of the Gabor-filter output under the assumption that the distribution is Rician. The estimated means and variances are used to establish a threshold that minimizes the image-segmentation error rate. Further, we consider the use of a post-filter in the analysis. The post-filter, which reduces the variance of the Rician-distributed Gabor-filtered output, results in a reduced image-segmentation error rate (at the expense of some resolution loss). The results in the final section demonstrate that the filter-design algorithm generates effective filters for image segmentation; moreover, the results show that our analysis accurately predicts filter-output statistics.

PROBLEM OVERVIEW

A block diagram of the fundamental signal processing under consideration is shown in Fig. 1. The technique outlined in the figure has been justified for texture segmentation by previous investigators [3, 5]. Below, we provide a signal-processing overview and define the filter-design problem.

The input image $i(x, y)$ is assumed to be composed of two textures and is first passed through a Gabor pre-filter with impulse response $h(x, y)$, where:

$$h(x,y) \quad = \quad g(x,y)\, e^{-j2\pi(Ux+Vy)} \qquad (1)$$

and,

$$g(x,y) \quad = \quad \frac{1}{2\pi\sigma_g^2}\, e^{-\frac{(x^2+y^2)}{2\sigma_g^2}} \qquad (2)$$

$h(x, y)$, referred to as a Gabor function, is a complex sinusoid, centered at frequency (U, V), modulated by a Gaussian envelope $g(x, y)$. Further, the 2-D Fourier transform of $h(x, y)$ is:

$$H(u,v) \quad = \quad G(u-U, v-V) \qquad (3)$$

where:

$$G(u,v) \quad = \quad e^{-2\pi^2\sigma_g^2(u^2+v^2)} \qquad (4)$$

is the Fourier transform of $g(x, y)$. The parameters (U, V, σ_g) determine $h(x, y)$. From (3-4), we see that the Gabor function is a bandpass filter centered about frequency (U, V), with bandwidth determined by σ_g. Also (1-2) indicate that σ_g determines the spatial extent of $h(x, y)$. (We assume for simplicity that the Gaussian envelope $g(x, y)$ is a symmetrical function.)

The output of the pre-filter stage $i_h(x, y)$ is the convolution of the input image with the filter response:

$$i_h(x,y) = h(x,y) ** i(x,y) \qquad (5)$$

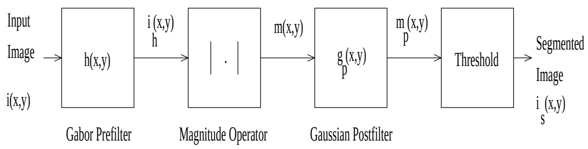

Figure 1. Signal processing block diagram.

The magnitude of the first-stage output is computed in the second stage (see [3, 5] for a justification of (6)):

$$m(x,y) = |i_h(x,y)| = |\ h(x,y) ** i(x,y)\ | \qquad (6)$$

Finally, a (low-pass) Gaussian post-filter $g_p(x,y)$ is applied to the magnitude output yielding the post-filtered image:

$$m_p(x,y) \quad = \quad m(x,y) ** g_p(x,y) \qquad (7)$$

where:

$$g_p(x,y) \quad = \quad \frac{1}{2\pi\sigma_p^2}\ e^{-\frac{(x^2+y^2)}{2\sigma_p^2}} \qquad (8)$$

Post-filtering (7) was used in [4] to smooth out variations in $m(x,y)$. This is discussed further in a later section. The final step, not shown in Fig. 1, is to segment the filtered image $m_p(x,y)$. To do this, we apply a threshold to $m_p(x,y)$; points above the threshold are assigned to one texture, and points below to the other.

Given the system of Fig. 1, we now state the Gabor pre-filter design problem. Consider the input image $i(x,y)$ composed of two dissimilar textures, $t_1(x,y)$ and $t_2(x,y)$. The problem is to find the Gabor function $h(x,y)$ that provides the greatest discrimination between the two textures in the filtered image $m_p(x,y)$.

Our approach to the problem is as follows. Using a statistical model for $i(x,y)$, find the Gabor function $h(x,y)$ that maximizes the output power ratio between the two textures in the pre-filter output $i_h(x,y)$. Then, upon applying a Gaussian post-filter, use the statistics of the output $m_p(x,y)$ to determine a threshold that minimizes the image-segmentation error in the final segmented image. The following two sections outline the analytical arguments and design procedures for our approach.

FILTER DESIGN ALGORITHM

In this section we propose a more efficient algorithm ($O(10N^2 log_2 N)$) than in [4] ($O(100N^2 log_2 N)$) for designing the Gabor pre-filter $h(x,y)$. The proposed method assumes that representative realizations of the two textures are available and draws upon the autocorrelations for each of the two sample textures. The statistics of $m(x,y)$ and $m_p(x,y)$ are discussed in the subsequent section, along with the effects of post-filtering.

Recall that the input image $i(x,y)$ is composed of two textures, $t_1(x,y)$ and $t_2(x,y)$. We assume that the given realizations of these two textures are samples from ergodic 2-D random processes. Denote the power spectral densities of $t_1(x,y)$ and $t_2(x,y)$ by $S_1(u,v)$ and $S_2(u,v)$. The subsequent analysis first considers the development for one texture, $t_1(x,y)$, and later generalizes the results to both textures.

When $t_1(x,y)$ is filtered by a Gabor pre-filter $h(x,y)$ with fixed parameters (U,V,σ_g), the total output power at $i_h(x,y)$ is:

$$P_1(U,V) \quad = \quad \int_{-\infty}^{\infty}\int_{-\infty}^{\infty} S_1(u,v)\ |G(u-U,v-V)|^2\ dudv \quad (9)$$

$P_1(u,v)$ can be calculated efficiently for all Gabor pre-filter center frequencies (U,V) simultaneously. To see this, consider a window $w(x,y)$ as follows:

$$w(x,y) = g(x,y) ** g(x,y) = \frac{1}{2\pi(\sqrt{2}\sigma_g)^2}\ e^{-\frac{(x^2+y^2)}{2(\sqrt{2}\sigma_g)^2}} \qquad (10)$$

where $g(x,y)$ is the Gaussian (2). Note that $w(x,y)$ is completely determined by parameter σ_g. From (2,4), the Fourier transform of $w(x,y)$ is:

$$\mathcal{F}\{g(x,y) ** g(x,y)\} = |G(u,v)|^2 = e^{-4\pi^2\sigma_g^2(u^2+v^2)} \quad (11)$$

where $\mathcal{F}\{\}$ denotes the Fourier transform operator. We now multiply the autocorrelation function $R_1(x,y)$ of the texture t_1 by the window function $w(x,y)$. The Fourier transform $\mathcal{F}\{\ w(x,y)R_1(x,y)\ \}$ of this windowed autocorrelation yields:

$$P_1(u,v) = \int_{-\infty}^{\infty}\int_{-\infty}^{\infty} S_1(\alpha,\beta)\,|G(u-\alpha,v-\beta)|^2\,d\alpha d\beta \quad (12)$$

From Parseval's theorem, $P_1(u,v)$ may be interpreted as the total output power of $i_h(x,y)$ for a Gabor pre-filter with center frequency (u,v) and parameter σ_g. This can also be seen by direct comparison of (9) with (12). Relation (12) can be efficiently implemented in a discretized form using the FFT. The discrete form then gives $P_1(u,v)$ at a discrete set of center frequencies (u,v) and a particular σ_g.

The foregoing analysis when applied to both textures, $t_1(x,y)$ and $t_2(x,y)$, leads to the filter-design algorithm summarized below:

1. Estimate the autocorrelations, $R_1(x,y)$ and $R_2(x,y)$, of the two textures of interest using the given realizations of the textures, t_1 and t_2.
2. Form the window function $w(x,y)$ in (10) for a given Gabor pre-filter parameter σ_g.
3. Compute $P_1(u,v)$ and $P_2(u,v)$ for the two textures using a discrete FFT implementation of (12).
4. Choose the center frequency that maximizes the ratio of $P_1(u,v)$ to $P_2(u,v)$ as follows:

$$(U,V) = arg\left\{\begin{matrix} max \\ (u,v)\end{matrix}\left(\frac{P_1(u,v)}{P_2(u,v)}\right)\right\} \quad (13)$$

5. Repeat steps 2 through 4 for all σ_g under consideration.
6. Select the Gabor pre-filter, specified by (U,V,σ_g), that gives the best segmentation error performance, based on criteria discussed in the next section.

The above algorithm gives a Gabor pre-filter that emphasizes texture t_1 over t_2 in the output i_h. An argument can be made for instead minimizing the power ratio in (13); *i.e.*, replace $arg\{max(\cdot)\}$ with $arg\{min(\cdot)\}$. This results in a filter that emphasizes t_2 over t_1, which could be a better filter. Finally, n textures can be considered instead of just 2, by making pairwise power ratio comparisons using (13).

The power ratio (13) is equivalent to the ratio of second moments of the pre-filtered outputs. In the absence of any additional information, the output variances and squared means should have the same ratio as the output powers. Thus, a large power ratio should correspond to lower classification error rates, since this implies that the ratio of the means for the two textures will be larger. Dunn and Higgins have shown that $m(x,y)$ in (6) has a Rician pdf for many textures [4]. The total output power, because of its statistical interpretation as the second moment, establishes upper bounds on the mean and variance of the Rician distributed pre-filter output magnitude $m(x,y)$.

FILTER OUTPUT STATISTICS

The previous section presented an efficient algorithm for designing the pre-filter $h(x,y)$. This section discusses how to estimate the statistics of $m(x,y)$ and $m_p(x,y)$ so that a threshold on $m_p(x,y)$ can be set that minimizes the image-segmentation error. An algorithm is developed to estimate the mean and variance of the outputs, $m(x,y)$ and $m_p(x,y)$, for each texture's expected Rician distribution. Once the output distributions for the two textures of interest are known, it is straightforward to calculate a threshold that minimizes image-segmentation error.

We first discuss a signal model that provides a framework for estimating the mean and variance of the pre-filter output magnitude $m(x,y)$ from the autocorrelation of a texture (or more precisely from an expression of the form (12)). Assume that $i_h(x,y)$ can be modeled approximately as a complex exponential signal $s(x,y)$ and a complex noise signal $n(x,y)$:

$$i_h(x,y) \approx s(x,y) + n(x,y) = A\,e^{-j2\pi(Ux+Vy)} + n(x,y) \quad (14)$$

The basic premise of (14) is that the pre-filter bandlimits the input such that the output $i_h(x,y)$ essentially consists of a small bandwidth around the center frequency (U,V) of the pre-filter. In many cases, the pre-filter focuses on a significant spectral peak of a texture. Thus, the output signal $i_h(x,y)$ in this small passband is then modeled as a single complex exponential plus complex bandpass noise. Strongly periodic components of a texture would tend to be represented by larger values of A.

The magnitude $m(x,y)$ of the complex signal $i_h(x,y)$ has a Rician distribution $p(m)$ when $n(x,y)$ is Gaussian bandlimited noise ; *i.e.*,

$$p(m) = \frac{2m}{N}\,e^{-(\frac{m^2+A^2}{N})}\,I_0(\frac{2mA}{N}) \quad (15)$$

where $m = m(x,y)$, A is the amplitude of the complex exponential, and N is the total noise power. The distribution is completely determined by the values of A and N.

When $A << N$, $p(m)$ approaches a Rayleigh distribution. This corresponds to the case where the filter output power is dispersed across the passband rather than being concentrated at the center frequency. Typically, the filter design algorithm tends to favor selecting $h(x,y)$ such that the filtered version of t_1 in $m(x,y)$ will be Rician, while the corresponding filtered version of t_2 in $m(x,y)$ will be approximately Rayleigh.

The model (14) permits the output statistics of $m(x,y)$ to be estimated from $P_1(u,v)$. Assume that the Gabor pre-filter passes spatial-frequencies localized around the center frequency (U,V) and rejects energy at other frequencies. Then a *locally* equivalent model in the spatial-frequency plane for an input texture $t_1(x,y)$ to the pre-filter is a power spectral density $S_1(u,v)$ consisting of a complex exponential plus white noise:

$$S_1(u,v) \approx A^2\delta(u-U,v-V) + \frac{\eta}{4} \quad (16)$$

We emphasize that this model is only valid within the approximate passband of the pre-filter. When the model (16) is applied to (12) of the filter design algorithm,

$$P_1(u,v) \approx A^2\,e^{-4\pi^2\sigma_g^2[(u-U)^2+(v-V)^2]} + \frac{\eta}{16\pi\sigma_g^2} \quad (17)$$

In (17) the first term arises from the sinusoidal term of (14). The second term represents the noise output power of the Gabor pre-filter, and gives the parameter N in (15): $N = \frac{\eta}{16\pi\sigma_g^2}$.

Given (17), the Rician parameters A and N may be estimated from $P_1(u,v)$. Denote the power for texture t_1 at pre-filter center frequency (U,V) as P_0. The half power point of $P_1(u,v)$ in the absence of noise occurs at a frequency offset of $\nu = \frac{.1325}{\sigma_g}$ (other offsets can be used). Then,

$$P_0 = P_1(U,V) = A^2 + N,$$
$$P_\nu = P_1(U\pm\nu,V) = A^2/2 + N \quad (18)$$

which gives relations for the Rician parameters:

$$A^2 \quad = \quad 2(P_0 - P_\nu), \quad N = 2P_\nu - P_0 \qquad (19)$$

Given A and N, the mean μ_g and variance s_g^2 of the Rician pdf characterizing $m(x,y)$ can be calculated. This is done for both sample textures using (U,V) from (13) and using $P_1(u,v)$ and $P_2(u,v)$ from (12) in place of $P_1(u,v)$ in (18).

Finally, an estimate is made for the output statistics of $m_p(x,y)$ under varying degrees of post-filtering. From (7) and (8) the post-filtering process can be considered as a spatial averaging of independent samples of $m(x,y)$. Under this assumption, the mean μ_p and variance s_p^2 of the post-filtered output can be approximated as:

$$\mu_p \quad = \quad \mu_g, \quad s_p^2 = \quad s_g^2\ \sigma_g^2/\sigma_p^2 \qquad (20)$$

For large ratios of σ_p^2/σ_g^2 , the post-filtered output pdf will become approximately Gaussian due to the central limit theorem. The image-segmentation threshold is then set assuming a bimodal Gaussian distribution with equal *a priori* probabilities for the two textures [8]. The effect of post-filtering is particularly pronounced as the ratio A/N becomes small. The Rician pdf approaches a Rayleigh pdf with small ratios of A/N. The longer tails on the Rayleigh distribution lead to large image-segmentation errors when post-filtering is not employed. The inclusion of post-filtering in the proposed methods enables a balanced treatment of Rician and Rayleigh distributed outputs.

The following is a summary of the algorithm for selecting a threshold and estimating the output distributions for the magnitudes of the Gabor pre-filter output, $m(x,y)$, and post-filter output, $m_p(x,y)$:

1. Obtain P_0 and P_ν from $P_1(u,v)$ and $P_2(u,v)$ using (18) with (U,V) from (13).
2. Calculate A and N for both textures using (19).
3. Estimate for each texture the pdf for $m(x,y)$ by substituting the estimates of A and N into (15). Calculate the means and variances of $m(x,y)$ for both textures.
4. Calculate post-filter output statistics using σ_p^2/σ_g^2 in (20), with the Gabor pre-filter output means and variances from step 3.
5. Set the image-segmentation threshold to minimize the error rate, given the distributions of the two textures and assuming equal *a priori* probabilities. In the post-filter case, the Gaussian assumption admits a closed-form solution for the threshold [8].
6. Repeat steps 4 and 5 for each σ_p^2 under consideration.
7. Choose the best compromise between the image resolution (determined by σ_p) and image-segmentation error (determined by σ_p^2/σ_g^2).

Note that the foregoing algorithm is not necessarily limited to the center-frequency (U,V) chosen by the frequency selection algorithm. However, by choosing a peak power point from (13), the frequency-selection algorithm tends to choose a center frequency that should be well represented by the presumed model (16).

RESULTS

Experiments were conducted on a range of Brodatz and synthetic texture images to test the filter-design algorithm and to test the output statistical estimates. Figure 2 presents segmentation results for a pair of Brodatz textures. The 256x256 input image $i(x,y)$ in Fig. 2a consists of a central d77 texture region superimposed on a background of the d16 texture. The pre-filter output magnitude $m(x,y)$ is shown in Fig. 2b. The measured histograms of $m(x,y)$ are shown in Fig. 2c as solid lines, and the predicted Rician pdf's using (15) are shown as dashed lines. The curves that peak at lower output amplitude correspond to the dark outer border (d16) of Fig. 2b, and the curves which peak at the larger amplitude correspond to the bright central region (d77) of Fig. 2b. The measured output statistics are seen to correspond well with the predicted Rician statistics. The results for a post-filter with $\sigma_p/\sigma_g = 2$ are shown in the second row of Fig. 2. The post-filtered output $m_p(x,y)$ is shown in Fig. 2d. The predicted Gaussian pdf (dashed lines) and measured output histograms (solid lines) are presented in Fig. 2e for the post-filtered image. The segmented image is shown in Fig. 2f for the post-filtered output.

The post-filtering reduces the tails of the measured histograms in Fig. 2. A large amount of overlap is seen in the pre-filter histograms of Fig. 2c. It is apparent that a segmentation without post-filtering will result in a large error rate. The histogram overlap is virtually eliminated by the post-filtering. This results in a low error rate for the binary segmentation of the image in Fig. 2f.

REFERENCES

[1] A. K. Jain and S. Bhattacharjee, "Text segmentation using Gabor filters for automatic document processing," *Machine Vision and Applic.*, vol. 5, pp. 169–84, 1992.

[2] A. K. Jain and F. Farrokhnia, "Unsupervised texture segmentation using Gabor filters," *Pattern Recognition*, vol. 23, no. 12, pp. 1167–86, Dec. 1991.

[3] A. C. Bovik, "Analysis of multichannel narrow-band filters for image texture segmentation," *IEEE Trans. Signal Processing*, vol. 39, no. 9, pp. 2025–43, Sept. 1991.

[4] D. F. Dunn and W. E. Higgins, "Optimal Gabor-filter design for texture segmentation," in *Proc. IEEE Int. Conf. Acoust., Speech, Signal Processing*, vol. V, pp. V37–V40, 1993.

[5] D. Dunn, W. Higgins, and J. Wakeley, "Texture segmentation using 2-D Gabor elementary functions," *IEEE Trans. Pattern Anal. and Machine Intell.*, vol. 16, no. 2, Feb. 1994.

[6] J. G. Daugman, "Uncertainty relation for resolution in space, spatial frequency, and orientation optimized by two-dimensional visual cortical filters," *J. Opt. Soc. Amer. A*, vol. 2, no. 7, pp. 1160–69, July 1985.

[7] A. C. Bovik, M. Clark, and W. S. Geisler, "Multichannel texture analysis using localized spatial filters," *IEEE Trans. Pattern Anal. Machine Intell.*, vol. 12, no. 1, pp. 55–73, Jan. 1990.

[8] R. C. Gonzalez and R. E. Woods, *Digital Image Processing.* Addison-Wesley, 1992.

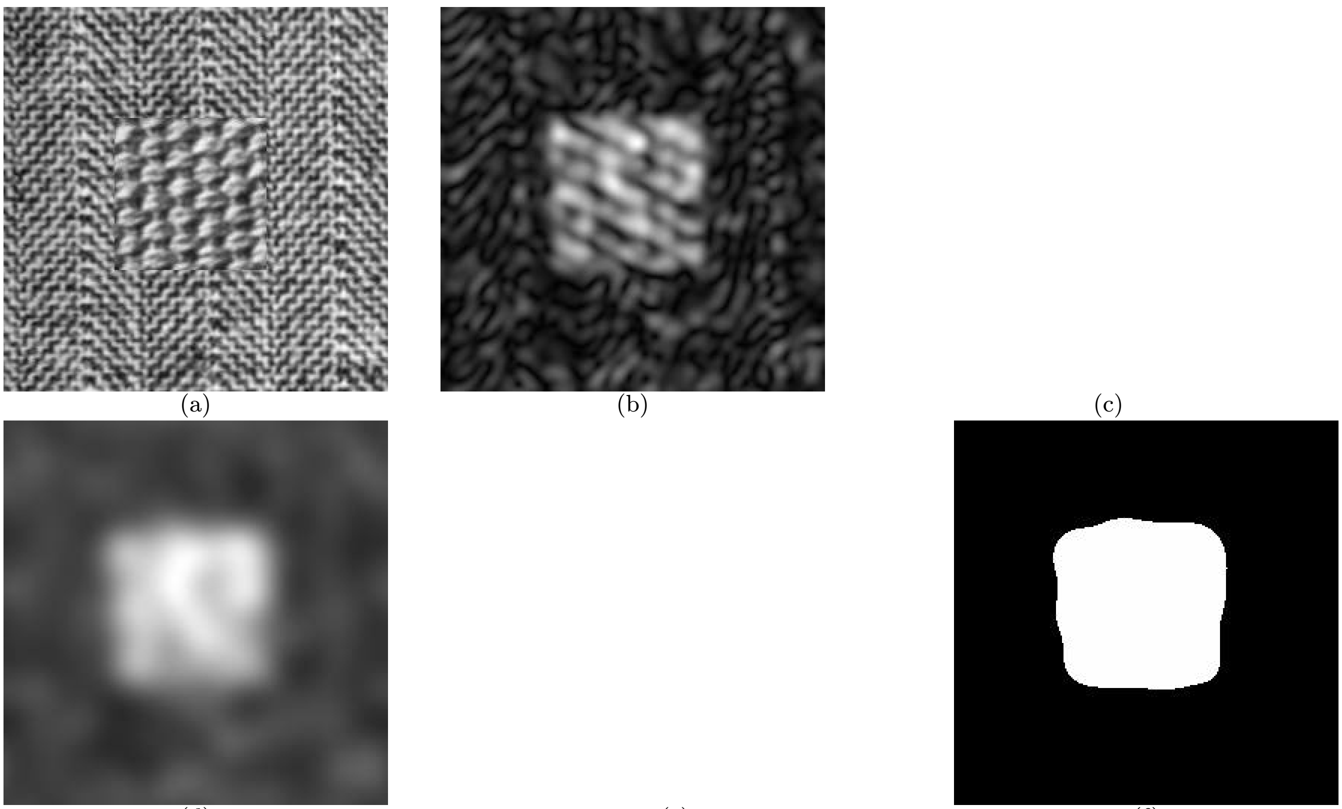

Figure 2. Gabor-filtered d16 "herringbone weave" (border) d77 "cotton canvas" (center) composite image, $\sigma_g = 5$, $(U, V) = (-.035, -.047)$ cycles/pixel. (a) Input image. (b) Magnitude of Gabor pre-filter output. (c) Histogram of Gabor pre-filter output magnitude, dash = predicted, solid = actual. (d) Post-filtered output, $\sigma_p = 2\sigma_g$. (e) Histogram of post-filtered output, $\sigma_p = 2\sigma_g$, dash = predicted, solid = actual. (f) Thresholded post-filtered image, $\sigma_p = 2\sigma_g$, threshold $= 10$.